Research Article

Selective Electrochemical Oxidation of H$_2$O to H$_2$O$_2$ Using Boron-Doped Diamond: An Experimental and Techno-Economic Evaluation

Kasper Wenderich,* Birgit A. M. Nieuweweme, Guido Mul, and Bastian T. Mei*

Cite This: ACS Sustainable Chem. Eng. 2021, 9, 7803–7812

Read Online

ACCESS | Metrics & More | Article Recommendations | Supporting Information

ABSTRACT: Selective water oxidation to hydrogen peroxide has emerged as an economically attractive replacement for oxygen in electrochemical hydrogen production by water splitting. Here, boron-doped diamond (BDD) is shown to be a promising anode material for anodic H$_2$O$_2$ formation. Faradaic efficiencies of up to 31.7% at 2.90 V versus the reference hydrogen electrode and a current density of 39.8 mA cm^{-2} were observed, corresponding to a H$_2$O$_2$ production rate of 3.93 μmol min^{-1} cm^{-2}. A techno-economic evaluation based on the experimentally obtained values demonstrates that the corresponding levelized cost of hydrogen (LCH) is significant ($62.0 kg^{-1}). Particularly, the current market price of BDD limits its implementation as a selective water oxidation anode for H$_2$O$_2$ generation. The sensitivity analysis however suggests that the LCH can be significantly improved by either decreasing the anode cost or increasing the current density. Both approaches are in fact feasible to allow for cost-effective electrochemical H$_2$ production and even competition with H$_2$ obtained from steam methane reforming. This study will guide ongoing research efforts toward BDD development and implementation of selective water oxidation to hydrogen peroxide.

KEYWORDS: boron-doped diamond, hydrogen peroxide, selective electrochemical water oxidation, techno-economic analysis, sensitivity analysis
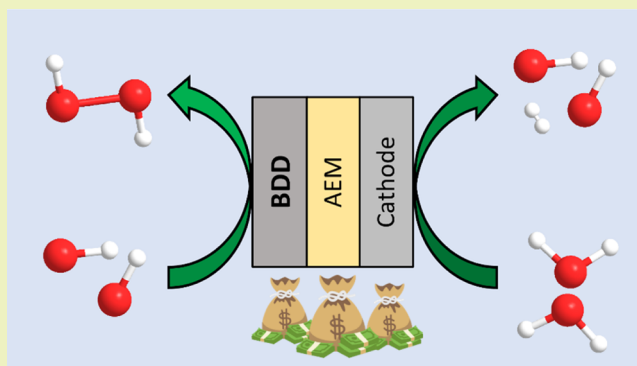
INTRODUCTION

Electrochemical water splitting driven by renewable energy sources is considered to be a promising carbon-free pathway for the production of the "green" fuel hydrogen.[1−3] Such electrochemical water splitting can be realized by water electrolysis powered by renewable electricity [e.g., photovoltaic (PV) cells or wind turbines][1,4−8] or alternatively by direct light utilization [e.g., using a photoelectrochemical (PEC) cell or photocatalysis].[9−11] Despite the promises of such an approach, the process economics are not yet favorable. Shaner et al. demonstrate that the levelized costs of hydrogen (LCHs) for photovoltaic electrolysis (PV-E) and PEC water splitting are $12.1 and $11.4 kg^{-1}, respectively.[1] More recently, Grimm et al. advocate LCH values of $6.22 and $8.43 kg^{-1} for PV-E and PEC, respectively,[8] thus indicating that PV-E is advantageous over PEC systems. Still, water electrolysis is not yet able to compete with the current price range of hydrogen obtained through steam methane reforming (SMR), with the latter corresponding to ~$1.4 kg^{-1}.[1,12]

Despite the fact that at the TW level, sustainable hydrogen production can only be accomplished through overall water splitting to hydrogen and oxygen, one of the major economic disadvantages of water electrolysis is the comparably low market value of co-produced oxygen ($35 ton^{-1}).[12] A recently suggested solution to lower the hydrogen price in water electrolysis is substitution of oxygen production by valuable chemical co-production in a paired electrolysis approach. Hydrogen peroxide (HP) is promising due to its high demand in the industry and its usage as an environmental-friendly oxidant.[13−16] A market value of $500 to $1200 ton^{-1} clearly indicates its financial benefits.[12] HP formation by selective oxidation of water occurs in alkaline media via eq 1[12,17]

$$2OH^- \rightarrow H_2O_2 + 2e^- \qquad E_0 = +1.78 \text{ V vs RHE} \qquad (1)$$
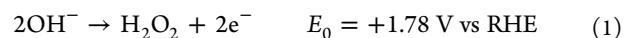
thus resulting in the overall water splitting reaction of

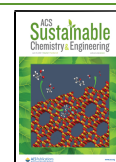$$2H_2O \rightarrow H_2O_2 + H_2 \qquad (2)$$

Electrification of H$_2$O$_2$ synthesis will allow for a sustainable replacement of the industrial anthraquinone oxidation (AO) process in a decentralized manner.[13−20] This will not only eliminate the need for harmful organic solvents in the synthesis
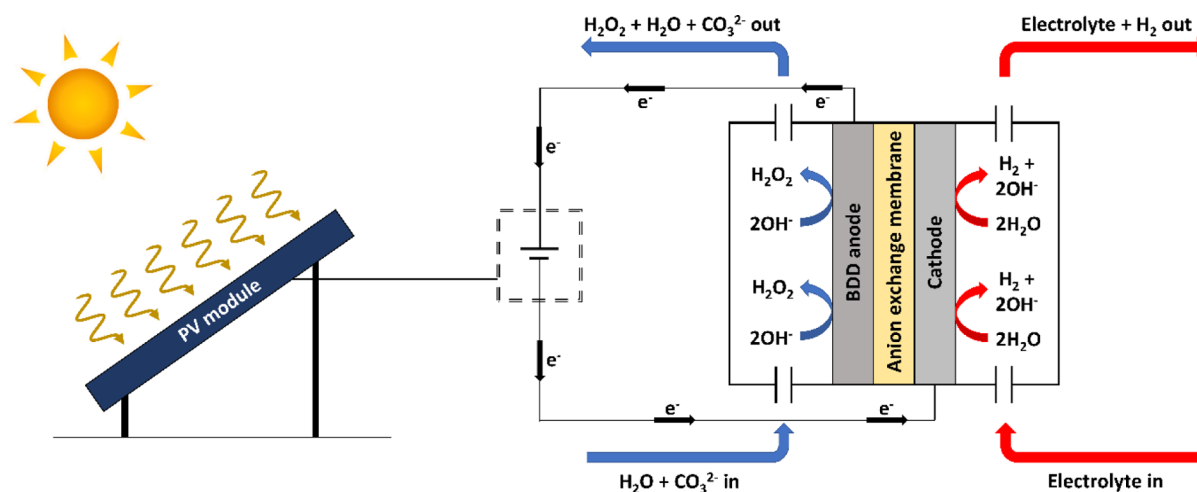
Figure 1. Schematic of a PV-E configuration which can be used for industrial selective water splitting to H_2 and H_2O_2. Photon energy is converted by a PV module into electrical energy, which is used to drive the oxidation reaction of hydroxyl ions to H_2O_2 on a BDD anode and to drive the reduction of water to H_2 on a suitable cathode. Water flows are used to harvest the products. Note that the image is not to scale: the area of the PV modules is much larger than the area of the electrolyzer. Furthermore, oxygen evolution will also take place at the anode in addition to H_2O_2 (not depicted. As implied by this study, FEs will be roughly 30 and 70% for H_2O_2 and O_2 production, respectively).

procedure but also reduce the requirement of the addition of stabilizers required for transportation of concentrated H_2O_2 solutions. Thus, the development of selective water oxidation to H_2O_2 will allow for dedicated H_2O_2 production facilities in a co-electrolysis manner.[21,22] Such H_2O_2 can then immediately be used on-site for, for example, bleaching in the pulp and textile industry or in a plant suited for treatment of wastewater or exhaust air.[13−16]

Electrochemical cathodic HP production from O_2 reduction has been investigated thoroughly and has been commercialized (e.g., *via* the Huron−Dow process).[15,23−26] In contrast, interest in anodic HP production has reappeared only recently.[15,16,21,27−31] Especially, metal oxides such as (modified) $BiVO_4$,[32−40] MnO_x,[41] $CaSnO_3$,[42] ZnO,[43] and C,N codoped TiO_2[44] have been reported as promising materials for selective H_2O_2 production, but germanium porphyrins[45] and aluminum porphyrins[46] have also been investigated. In electrochemistry, carbon-based materials have been widely employed.[47−50] Especially, boron-doped diamond (BDD) is alluring to study due to its robustness.[47,50] Although carbon electrodes have not been investigated thoroughly yet for anodic H_2O_2 production, the recent literature suggests BDD to be an outstanding anode material.[51] Here, Faradaic efficiencies (FEs) of up to 28% [at 3.17 V vs reference hydrogen electrode (RHE), in 2 M $KHCO_3$, estimated to correspond roughly to a H_2O_2 production rate of 11 μmol min^{-1} cm^{-2}] have been reported. In another study, Xia et al. focused on polytetrafluoroethylene (PTFE)-coated carbon fiber paper (CFP).[22] With a production rate of 23.4 μmol min^{-1} cm^{-2} H_2O_2 (at 2.4 V vs RHE) and FEs of up to 66%, these carbon-based electrodes appear to be promising for anodic H_2O_2 production, but the long-term durability has yet to be revealed.

Here, we experimentally confirm that BDD is a promising material for anodic H_2O_2 production. Particularly, it is shown that the FE can be further improved using sodium carbonate (Na_2CO_3) as an electrolyte. Using our experimental data as input, we performed a techno-economic analysis for an off-grid PV-E system for coupled electrochemical H_2/H_2O_2 generation. Furthermore, we performed a thorough sensitivity analysis of the system to investigate the dependence of the LCH (i.e., the

minimum price at which H_2 needs to be sold for the process to be profitable) as a function of anode costs, H_2O_2 price, and PV module costs. Our analysis suggests that processes enabling H_2 production at costs similar to those of SMR are feasible if the cost of BDD is reduced and partial current densities toward H_2O_2 are improved.

■ METHODOLOGY

Experimental Section. The experimental section is described in detail in the Supporting Information.

Techno-Economic System Design. Economic evaluation of the suitability of BDD has been performed, following recently reported techno-economic evaluations performed by this group.[52] A PV-E cell is used, in which silicon-based PV modules are utilized to harvest solar light. BDD is used as an anode material allowing for simultaneous hydrogen peroxide evolution and oxygen evolution. For cathodic hydrogen evolution, platinum electrodes are considered. An anion-exchange membrane (AEM) is assumed to separate the compartments and to facilitate ion transport. A liquid electrolyte flow containing carbonate, Na_2CO_3 here, is included in the anodic compartment. Water streams are proposed to harvest the products of interest, that is, hydrogen and HP. For future applications, a membrane electrode assembly (MEA) configuration with gas streams for harvesting at the cathode could be considered as well. A schematic depiction of the principle of the setup is shown in Figure 1, and the considered industrial process is depicted in Figure S3.

Cathodically produced H_2 is separated from the catholyte, after which the liquid electrolyte is recycled. The hydrogen is compressed and stored. The output at the anode side will, apart from water and CO_3^{2-}, consist of HP and oxygen. An important aspect to consider is that H_2O_2 is not stable under alkaline conditions.[15,17,53] For immediate on-site use of H_2O_2, stabilization is not required. However, for H_2O_2 storage, acidification is necessary. For long-term storage also, the addition of a stabilizer might be required. Carbonate present in the anolyte will react to CO_2 which can be captured and recycled by alkalinization. Depending on the application of the PV-E plant, further water evaporation for a higher H_2O_2

concentration is possible as well. A 100% efficiency in the separation of chemicals is assumed in this work.

Techno-Economic Assumptions. The most important techno-economic parameters are summarized in Tables 1 and

Table 1. Parameter Assumptions for a PV-Driven H_2/H_2O_2 Electrolysis Cell with BDD as an Anode

parameter	value
H_2 production scale[1,8,54,55]	10 t H_2 d^{-1}
solar energy input[8,54,55]	6.19 kW h m^{-2} d^{-1}
daily operating time	12 h
starting year	2022
project lifetime[1,8,54,55]	20 years
PV replacement time[1,8]	20 years
electrolyzer stack replacement time[1,8]	7 years
PV efficiency[56]	18.6%
capacity factor[8]	90%
inflation rate[1,8]	1.9%
tax rate[55]	38.9%
discount rate[55]	10%
H_2O_2 price range	$0.5–2.5 kg^{-1}
H_2O_2 base-case price	$1.5 kg^{-1}

2. Most values are adapted from previous work performed in our group (and also in line with other techno-economic studies on "classic" PEC water splitting).[52] Here, it is assumed that the off-grid PV-E plant is located in Daggett, California, USA, and allows for production of 10 ton of H_2 per day.[8,54,55] The solar panel array will be tilted to the south under an angle of 35°. Thus, an average solar energy input of 6.19 kW h m^{-2} d^{-1} is considered. The daily operating time is 12 h at an efficiency of 18.6%.[56] The PV-E lifetime is considered to be 20 years, and no replacement of the PV cell is required within this period.[1,8] The default electrolyzer stack replacement time is 7 years.[1,8]

In this article, the H_2O_2 price range, the PV module cost range, and the cost range of the BDD anode are investigated in detail. On the basis of an estimated H_2O_2 price range of $0.5–$1.2 kg^{-1} from 2006[12,52,57] and taking into account a possible inflation rate of *ca.* 1.9%,[1,8] we roughly estimate the price range in this study to be in the range of $0.5–2.5 kg^{-1} with a base-case value of $1.5 kg^{-1}. The PV module cost range ($0.150–0.300 W^{-1}, base-case $0.179 W^{-1}) and PV module efficiency are based on the costs for 275–280/330–335 W Multi Modules as assessed on EnergyTrend.[56] The additional wiring and mounting costs are calculated to be 28.2 and 41.0% of the sole PV module costs, respectively.[58] It is assumed that the PV modules are directly connected to the electrolyzer and that no DC−DC converter is required (a DC−DC converter will allow for optimal operation at all times but adds additional costs; it is expected that efficiency losses due to non-optimized performance will be similar to efficiency losses caused by the DC−DC converter).[1,8] The anode cost of BDD is very uncertain and is therefore investigated for a broad range. As the base-case cost is estimated to be $26,500 m^{-2},[59] the upper limit in this range was defined at $100,000 m^{-2}. The lower limit is set at $1 m^{-2}, in accordance with the cost range of anodes used in previous techno-economic studies.[1,8,52] Considering ongoing improvements in the synthesis of BDD and the economy of scale, BDD costs are expected to decrease significantly. Ground costs ($0.15 m^{-2}) are considered to be negligible.[8,52,55] Finally, it should be noted that various parameters included in this study are country-/location-dependent.

Table 2. Economic Costs Used in a PV-Driven H_2/H_2O_2 Electrolysis Cell with BDD as an Anode

parameter	value
CAPEX	
PV Configuration	
PV module cost range[56]	$0.150–0.300 W^{-1}
PV module base-case cost[56]	$0.179 W^{-1}
wiring (adapted from ref 58)	28.2% of the PV module price
mounting (adapted from ref 58)	41.0% of the PV module price
Electrolysis Module	
housing (adapted from refs 8 and 52)	$28 m^{-2}
cathode (adapted from ref 1)	$5 m^{-2}
membrane[1,8]	$50 m^{-2}
assembly[8]	$20 m^{-2}
anode (BDD) cost range	$1–10^5 m^{-2}
anode (BDD) base-case cost[59]	$26.5 × 10^3$ m^{-2}
electrolysis module replacement costs	75% after 7 years and 60% after 14 years
Hard BoS	
H_2 gas system (including gas compressors, piping, condensors, and intercooling)[8]	M$11.5
H_2O piping system[52] (adapted from ref 8)	M$2.6
H_2O_2 piping system[52]	M$2.6
electrolyte, H_2O_2 and H_2O separator[52]	M$5
process control system[52]	M$6
Soft BoS	
installation costs[8]	20% of initial investment + replacement costs
contingency costs[8]	30% of initial investment
engineering and design costs[8]	5% of initial investment
OPEX	
insurance[8,55]	2% of initial CAPEX of the electrolysis module, PV configuration, and hard BoS a^{-1}
labor[52]	M$4.5 a^{-1}

A flow chart of the economic model used is provided in Figure S4.[52] Briefly, the model is based on calculating the requirements to achieve a net present value (NPV) of 0, which corresponds to the economic break-even point.[1,8,52] The NPV is dependent on the yearly cash flow, the discount rate, and the project lifetime. A mathematical description of the NPV calculation can be found both in the Supporting Information and in previous work.[52] For detailed calculations on the required area of the electrolyzer, the required area of PV modules, and the amount of H_2O_2 produced, we also refer to the Supporting Information.

EXPERIMENTAL RESULTS AND DISCUSSION

The electrochemical properties of BDD electrodes for selective water oxidation to HP were investigated using either 1 M Na_2CO_3 or 1 M $NaHCO_3$ as an electrolyte (for further details regarding the experimental procedures, see the Supporting Information). Comparison of the two electrolytes revealed that the obtained FEs for HP formation are beneficial in 1 M Na_2CO_3 (Figure S5). In the literature, it is often advocated that bicarbonates are essential to achieve selectivity in water oxidation to H_2O_2.[32,33] Just recently, however, Xia et al. reported for PTFE-coated CFP electrodes that 1 M Na_2CO_3 is preferred over 1 M $NaHCO_3$, in agreement with this study.[22] Therefore, 1 M Na_2CO_3 is used as an electrolyte to determine the required input parameters for the techno-economic evaluation. The cyclic voltammogram as well as the FE, the H_2O_2 evolution rate, and
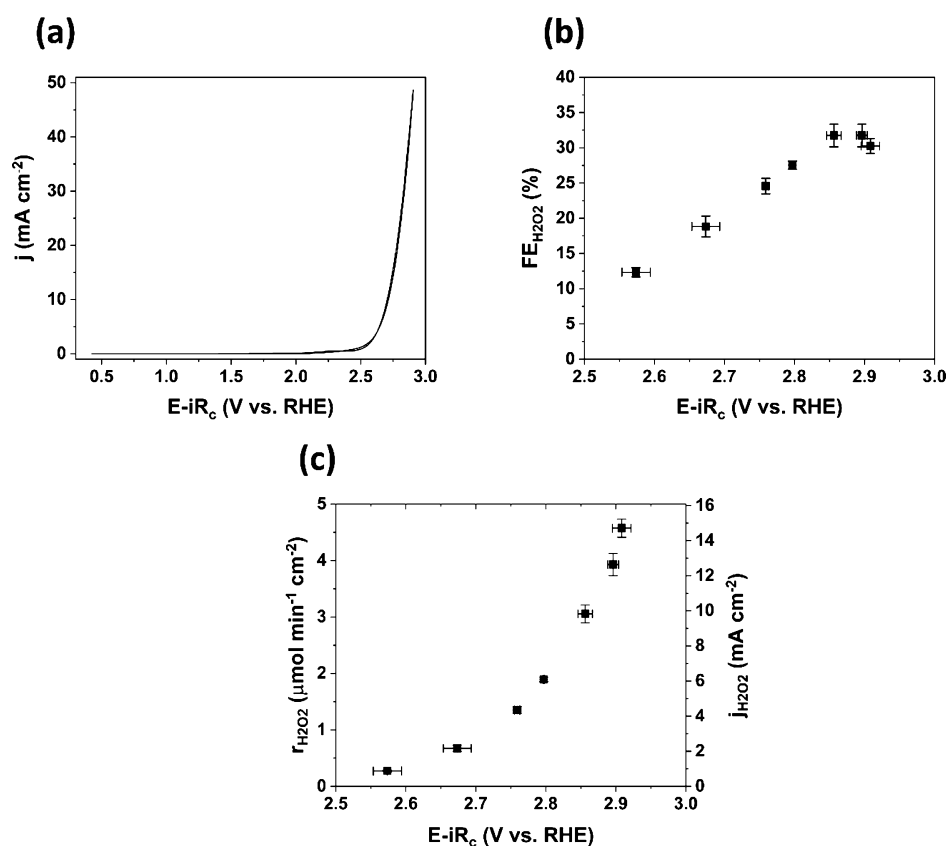
Figure 2. (a) Cyclic voltammetry (CV) curve of BDD electrodes on a niobium substrate measured in 1 M Na_2CO_3 with a Ag/AgCl (3 M NaCl) reference electrode and a Pt counter electrode. (b) FE as a function of applied voltage. (c) H_2O_2 production rate and partial current density as a function of the applied voltage. Note that data in (b,c) have been corrected for H_2O_2 degradation (see Figure S2 for further information).

the H_2O_2 partial current density obtained with BDD anodes are depicted in Figure 2. The onset potential for water oxidation is defined to be 2.1 V versus RHE at 0.2 mA/cm^2 (using the forward scan), corresponding to an overpotential of at least 320 mV for HP production. The optimal FE is found to be of 31.7% at 2.90 V versus RHE, resulting in a production rate of 3.93 μmol min^{-1} cm^{-2}. It should be noted that a non-optimized simple batch reactor was used in this study. Optimization of the reactor and transport will likely enable operation with even improved performance.

Compared to other materials, BDD anodes used in this study also perform well. For example, when comparing to $BiVO_4$ anodes reported by Shi et al.,[33] higher H_2O_2 production rates were observed in this study for potentials ≥2.8 V versus RHE. Moreover, the current onset potential reported here is shifted negative compared to the results reported by Mavrikis et al.,[51] possibly caused by the lower conductivity and the resulting higher resistance of the HCO_3^- electrolyte used by the latter. It is also shown that selective water electrolysis to H_2O_2 on BDD anodes yields higher FEs when used in carbonate-containing electrolytes. Still, PTFE-coated CFP anodes reported by Xia et al.[22] outperform BDD. It is important to note though that the electrochemically active surface area of BDD used here is considerably smaller than that for CFP. The stability of BDD, however, is expected to be a main advantage as other carbon-based electrodes are known to be unstable at oxidative potentials.[60,61] Still, in ongoing studies using BDD as anodes, use of hydrophobic coatings should be considered to further improve the selectivity to HP.

As stated, a major advantage of BDD over other types of anode materials for HP production is its robustness and stability.[47] To get an indication of the stability of BDD anodes during electrochemical water oxidation, we determined the double-layer capacitance of BDD prior to each measurement. For a detailed description on the determination, we refer to the Supporting Information (Figures S6 and S7).[62,63] Although the error margin is relatively large in our

experiments, there is no increase in real surface area of the electrodes. It could even be argued that the capacitance slightly decreases over the first six chronopotentiometry measurements performed, after which it stabilizes. A possible explanation of the observed behavior is the oxidation of initially present sp^2 carbon and its removal.[61] Scanning electron microscopy (SEM) images also demonstrate that BDD is stable throughout the measurements (Figure S7). We find that the behavior of the chronopotentiometry measurements did not change significantly overtime (Figure S8). Therefore, we considered BDD to be a stable electrode material after initial surface activation, in agreement with the literature and thus suitable for implementation at the industrial scale.[61]

TECHNO-ECONOMIC ANALYSIS RESULTS AND DISCUSSION

Techno-Economic Evaluation of Experimental Data. To proceed with the evaluation of BDD anodes used in co-electrolysis of H_2 and H_2O_2 at the industrial scale, the following initial assumptions were made: (i) the results of the batch reactor can be translated to a flow system; (ii) the maximum achievable FE for HP with BDD anodes is 31.7%; (iii) to achieve a current density of approximately 100 mA/cm^2, a cell potential of *ca.* 3.7 V is required (see Figure S9); (iv) the stability of the BDD allows for continuous operation for 7 years; and (v) the FE toward H_2 at the cathode is 100%. Although BDD has been around for several decades,[47] full commercialization of BDD has not yet been achieved. As of 2014, only five companies selling BDD were reported,[61] and the costs per unit of area are still relatively high. Here, we estimate the base-case BDD cost to be 26.5×10^3 m^{-2}.[59] Considering the described boundaries, the anode costs were

identified to be the main bottleneck for commercial implementation of anodic H_2O_2 production using BDD electrodes. Current limited availability and future large-scale production suggest that a significant drop in BDD costs can be expected. Thus, in the following, a hydrogen cost analysis as a function of anode costs and H_2O_2 price (Figure 3a) or PV
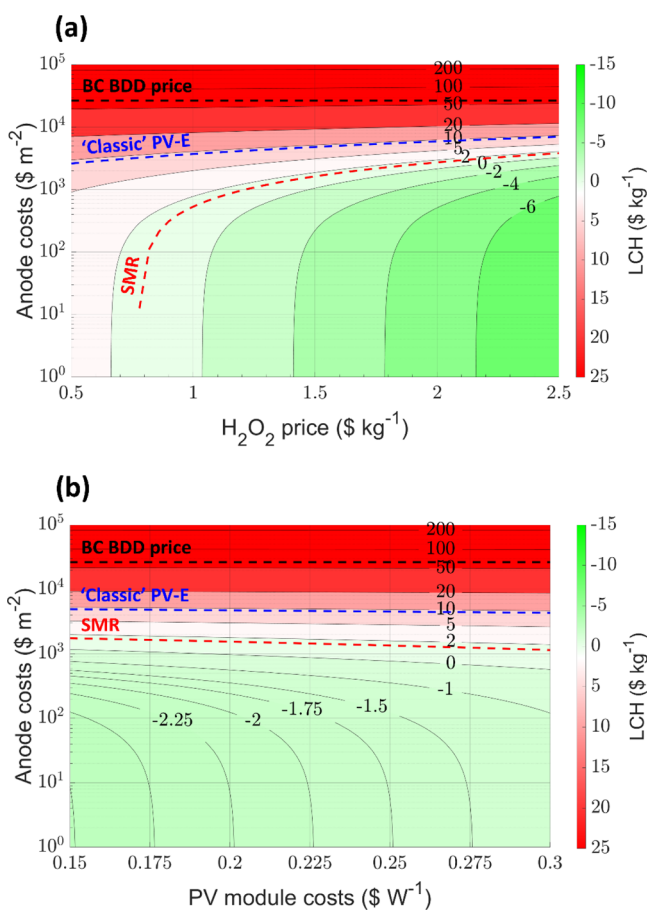

Figure 3. LCH as a function of anode costs and (a) H_2O_2 price and (b) PV module costs using parameters defined in Tables 1 and 2 and using a current density of *ca.* 100 mA/cm^2, a voltage of *ca.* 3.7 V, and an FE of 31.7%. The black solid line indicates the estimated base-case costs of BDD. The blue dotted line is a representation of the estimated LCH for "classic" PV-driven electrolysis ($9.16 kg^{-1}),[1,8] whereas the red dotted line corresponds to the LCH produced by SMR ($1.4 kg^{-1}).[1,12] The base-case values used are (a) $0.179 W^{-1} for the PV module costs and (b) $1.5 kg^{-1} for the H_2O_2 price.

module costs (Figure 3b) is reported. As can be seen, for example, from Figure 3a (very light-red area), at a H_2O_2 price of $1.5 kg^{-1} and at an anode cost of $1000 m^{-2}, the LCH is in the range of $2−5 kg^{-1} (at 0.179 $ W^{-1} for the PV module costs). In addition, Figure 3b shows that at a BDD cost of ~$2500 m^{-2} and a H_2O_2 price of $1.5 kg^{-1}, the cost of hydrogen would be in the same range of $2−5 kg^{-1}, rather independent of the cost of the PV module (in $ W^{-1}). The most important values from Figure 3 are also summarized in Tables 3 and 4.

It is very clear that the anode costs have a quite obvious effect on the LCH. At high anode costs, the influence of the H_2O_2 price and the PV module costs is negligible, and only for BDD anode costs below $5000 m^{-2}, a clear dependence of H_2O_2 price and PV module costs is observed.

Table 3. Most Important LCH Values as a Function of H_2O_2 and Anode Costs as Derived from Figure 3a for a PV-E System with a Current Density, a Voltage, and an FE of *ca.* 100 mA/cm^2, *ca.* 3.7 V, and 31.7%, Respectively

H_2O_2 price ($ kg^{-1})	anode costs (10^3 $ m^{-2})	LCH ($ kg^{-1})
0.5	26.5	67.4
	2.62	9.16
	0.01	2.89
1.5	26.5	62.0
	4.81	9.16
	1.63	1.4
2.5	26.5	56.7
	7.01	9.16
	3.82	1.4

Table 4. Most Important LCH Values as a Function of PV Module and Anode Costs as Derived from Figure 3b for a PV-E System with a Current Density, a Voltage, and an FE of *ca.* 100 mA/cm^2, *ca.* 3.7 V, and 31.7%, Respectively

PV module price ($ W^{-1})	anode costs (10^3 $ m^{-2})	LCH ($ kg^{-1})
0.150	26.5	61.8
	4.93	9.16
	1.75	1.4
0.179	26.5	62.0
	4.81	9.16
	1.63	1.4
0.300	26.5	63.2
	4.33	9.16
	1.15	1.4

To be competitive with the "classic" H_2/O_2 PV-E water splitting approach,[1,8] the BDD costs should drop below $4.81 × 10^3 m^{-2}$. At $1.63 × 10^3 m^{-2}$, the calculated LCH is competitive with current hydrogen market values (obtained through SMR).[1,12] For comparison, the industrial price of dimensionally stable anodes (DSAs) is estimated to be roughly $3500 m^{-2}$,[64] underlining that lower BDD prices (i.e., in the order of magnitude of $1−5 × 10^3 m^{-2}$) can be achieved in the future by scaling BDD production. Considering the dependence of the LCH on the H_2O_2 price, it is important to note that even for low anode costs, a minimum H_2O_2 price is required to allow for competition with hydrogen production *via* SMR. Based on this base-case scenario calculations, the minimum H_2O_2 market value is approximately $0.78 kg^{-1}. This minimum required H_2O_2 price decreases when the current density increases, although the effect is minor (e.g., over $0.74 kg for 500 mA cm^{-2}).

Cost Comparison and Sensitivity Analysis. We proceed to evaluate the dependence of the LCH as a function of input parameters used in this study. First, we break down the CAPEX and OPEX costs of the system (Figure 4a) and perform a sensitivity analysis to elucidate the influence of the CAPEX and OPEX costs on the LCH (Figure 4b). We conclude that the CAPEX costs are more than 4.5 times higher than the OPEX costs in the described scenario, and 72% of the CAPEX costs are attributed solely to the electrolysis cell. While this is not surprising, considering the estimated costs of the BDD anode, it is worth noting that the area of the electrolysis cell is considerably smaller than the area of the PV modules used: $26.8 × 10^3 m^2$ versus $1.05 × 10^6 m^2$. Consequently, reduction of the CAPEX costs has a far larger influence on the
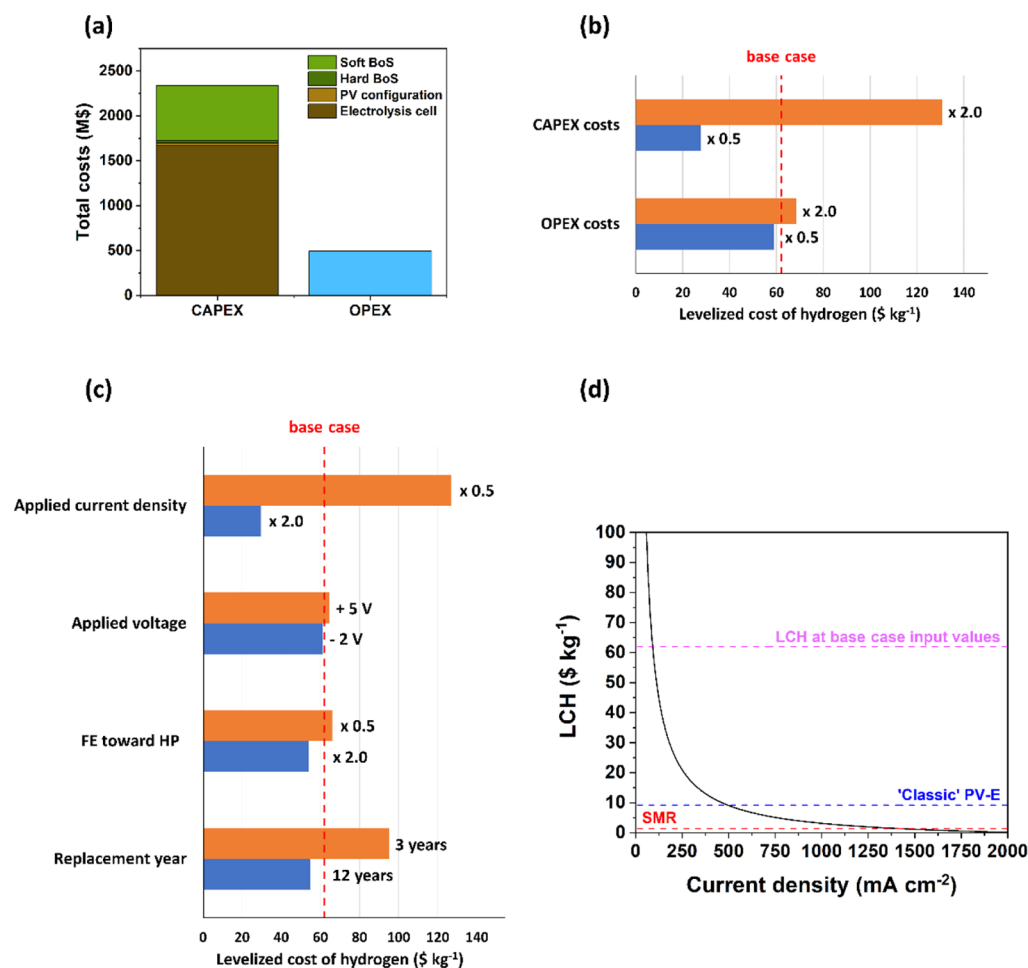
Figure 4. Sensitivity analysis of a PV-E system using parameters defined in Tables 1 and 2 and using a current density of *ca.* 100 mA/cm², a voltage of *ca.* 3.7 V, and an FE of 31.7%. (a) Breakdown of the CAPEX and OPEX costs. (b + c) LCH as a function of a modification in (b) CAPEX and OPEX costs and (c) applied current density, applied voltage, FE toward H_2O_2 evolution, and the replacement year. (d) LCH as a function of current density. Dotted lines indicate the LCH value found when a current of 91.8 mA/cm² is applied (pink), with the LCH value corresponding to "classic" PV-E water splitting (blue) and the LCH value corresponding to SMR (red). Note that the voltage is kept constant for this situation.
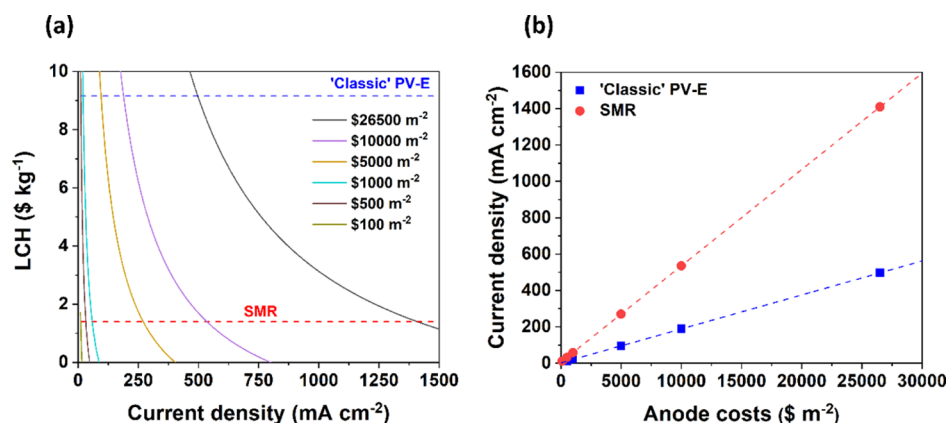

Figure 5. (a) LCH as a function of current density at different anode costs. Dotted lines indicate the LCH value corresponding to "classic" PV-E water splitting (blue) and the LCH value corresponding to SMR (red). Note that the voltage is kept constant for this situation. (b) Current density required to financially outperform "classic" PV-E water splitting or SMR as a function of anode costs. The dotted lines represent a linear fit.

LCH than reduction of the OPEX costs, as highlighted in Figure 4a,b. Specifically, the CAPEX costs associated with the electrolysis cell should be decreased.

The sensitivity of the LCH was also analyzed for its dependance on the applied current density, the applied cell voltage, the electrode stability, and the FE toward H_2O_2. The results are summarized in Figure 4c. As demonstrated in our previous study,[52] it is important to aim for a high replacement time. Although there is only a small decrease in LCH when the replacement time increases to 12 years (from $62.0 to $54.8
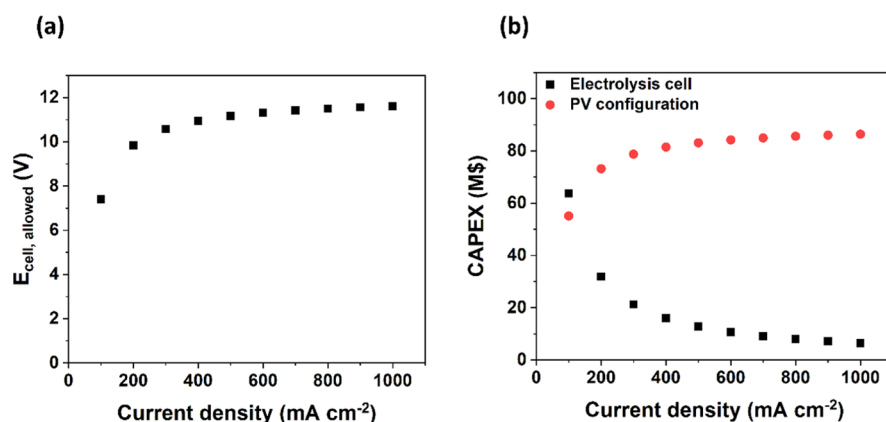
Figure 6. (a) Maximum cell potential allowed without exceeding anode costs of *ca.* $1000 m^{-2} as a function of current density. (b) Corresponding CAPEX values of the electrolysis cell and the PV configuration with anode costs of *ca.* $1000 m^{-2}.

kg^{-1}), a significant increase is observed when the replacement time is lowered to 3 years (from $62.0 to $95.1 kg^{-1}). Although there is only a mediocre impact of the FE on the calculated LCH, the influence of the current density is significant. This is easily understood by the relation of current density and required anode area to produce the same quantities of H_2O_2 and H_2, and thus, a significant decrease of the total CAPEX can be achieved.

Remarkable is the very small contribution of the applied voltage on the LCH. This voltage is dependent on the power output of the PV module, which has a low cost compared to the electrolysis cell. Practically, this implies that increasing the voltage to obtain higher current densities is feasible, provided that other process limitations, for example, intensive bubble formation at the electrode surface, are avoidable. However, it should be noted that when current densities are increased, the cost ratio of the PV configuration/electrolyzer stack increases. Thus, even if the LCH decreases with increasing current densities, its voltage dependence will increase (in terms of percentage).

In Figure 4d, we further evaluate the LCH as a function of current density. When the current density is increased from 91.8 mA/cm^2 to 1 A/cm^2, the LCH is reduced significantly from $62.0 to $3.13 kg^{-1}, and already at 497 mA cm^{-2}, the H_2/H_2O_2 process will outperform "classic" water splitting despite the significant costs of BDD. The break-even point for competition with hydrogen produced through SMR is only achieved at 1.41 A cm^{-2}, implying that industrially relevant current densities for cost-competitive H_2/H_2O_2 electrolysis must be achieved. Obviously, the current densities required to financially outperform hydrogen production from "classic" PV water splitting or SMR decrease when the anode costs decrease. For instance, at $10,000 m^{-2}, these current densities are 189 and 535 mA cm^{-2}, respectively, and at a BDD cost of $1000 mA cm^{-2}, a significant drop in current densities to 20.6 and 58.4 mA cm^{-2} (see Figure 5) is calculated.

To purely highlight the large influence of the current density in Figure 4d, no cell potential change was taken into account yet. Although an increase in current density will result in a decrease in the costs of the electrolyzer stack, the costs associated with the required PV system will increase due to the higher power output required. To be able to discuss the voltage dependence on the LCH, we estimate the maximum allowed voltage to enable hydrogen production at a cost of $1.4 kg^{-1} (in agreement with SMR) without exceeding an

anode cost of *ca.* $1000 m^{-2}. The results are depicted in Figure 6a. For small current densities (<400 mA cm^{-2}), the maximum allowed voltage is increasing. For current densities larger than 500 mA cm^{-2}, however, the maximum allowed cell potential is limited to approximately 11 V. Thus, the associated PV costs become relatively more dominant in the total process cost evaluation, and in fact, economic production is limited to a maximum cell potential of 11 V. Indeed, the CAPEX values for the electrolyzer stack and the PV configuration for low applied cell potentials are initially in the same order of magnitude (Figure 6b), with the latter becoming more dominant at ≥200 mA cm^{-2} following the trend observed for the maximum allowed cell voltage. The ratio between the CAPEX costs increases linearly with an increasing current density (Figure S10). From these data, it can be concluded that increasing the current density is a sound approach in suppressing the costs for the electrolyzer stack, provided that the voltage does not exceed a calculated limiting potential value, with the latter being relatively high and therefore likely not to be exceeded.

Further sensitivity analysis on the cathode costs, the membrane costs, and the capacity factor is reported in Figure S11 (although the influence of these parameters is not large). For the sensitivity analysis on more general trends such as the influence of solar energy input or tax rate, we refer to earlier published work.[52]

Future Prospects. To allow for feasible implementation of BDD in a H_2/H_2O_2 PV-E system, future experimental work should aim at increasing the H_2O_2 production rate and the BDD stability and/or suppressing the BDD costs. For example, Mavrikis et al. have already demonstrated that at higher voltages, a production rate of 19.7 μmol min^{-1} cm^{-2} can be achieved.[51] A strategy to decrease the costs of the BDD anode is to replace the substrate used for synthesis. Here, a niobium substrate was utilized; however, with the use of a silicon substrate, a significant drop in anode costs is envisioned. Besides the lower costs of the substrate, BDD processing also simplifies. While a two-sided coating is required on a niobium substrate to prevent bending,[59] stable single-side coatings can be used on silicon substrates. Initial state-of-the-art experiments have already been performed in our group, demonstrating that BDD on silicon substrates is suitable for anodic production of H_2O_2. Future research should be aimed at obtaining or even exceeding the same H_2O_2 production rates and FEs with convincing stabilities using such BDD-coated silicon substrates.

Alternatively, also, other carbon-based materials could be investigated for their suitability in anodic H_2O_2 production. A good example of such a material would be the PTFE-coated CFP used by Xia et al. (also see the Introduction).[22] For PTFE-coated CFP, excellent FEs and H_2O_2 production rates were determined and extended stability for several hours was revealed. In addition, the costs associated with PTFE-coated CFP are roughly a factor of 10−50 lower than the current base-case costs of BDD (depending on the amount of PTFE coated).[65] The stability is remarkable as CFP likely consists of sp^2-carbon and oxidation is expected at potentials relevant for HP synthesis.[61,66] BDD being mainly carbon in sp^3-hybridization should be favorable in this respect. A current density of 720 mA cm^{-2} has in fact been reported with BDD showing good corrosion conditions.[67] For further verification for the suitability in industrial applications, long-term stability tests are required for both PTFE-coated CFP and BDD.

Finally, it is important to realize that the general trends observed here in the context of hydrogen production by water electrolysis can be translated into other electrochemical processes of interest. Examples include (but are not limited to) CO_2 reduction, nitrogen fixation, and selective oxygen reduction to H_2O_2.

CONCLUSIONS

In this article, BDD was investigated on both an experimental level and a techno-economic level for its (commercial) suitability as an anode material in an electrochemical H_2/H_2O_2 process. Utilizing sodium carbonate as an electrolyte, H_2O_2 FEs of up to 31.7% at 2.90 V versus RHE with a production rate of 3.93 μmol min^{-1} cm^{-2} were determined. Despite the promising nature of BDD in terms of H_2O_2 production rates and stability, the performed techno-economic analysis revealed that the current market value of BDD impedes its implementation in a H_2/H_2O_2 PV-E plant. By means of a sensitivity analysis, we demonstrate that the best approach to reach financial competitiveness with SMR for the production of H_2 is either by lowering the anode costs or by increasing the production rates, that is, current densities. In the latter case, care should be taken not to exceed a limiting maximum potential provided by the PV module.

ASSOCIATED CONTENT

Ⓢ Supporting Information

The Supporting Information is available free of charge at https://pubs.acs.org/doi/10.1021/acssuschemeng.1c01244.

> Experimental details; mathematical calculations; schematic of the electrochemical cell used; explanation on H_2O_2 degradation correction; schematics of the industrial PV-E process modelled and a flow chart demonstrating the principles of the model; CV scans comparing usage of 1 M Na_2CO_3 versus 1 M $NaHCO_3$; explanation and results of electrode capacitance determination; SEM images of BDD before and after experiments; examples of chronopotentiometry curves; CV scan of a two-electrode configuration; CAPEX ratio between the PV configuration and electrolysis cell as a function of applied current density; further sensitivity analysis; and Matlab files used for modelling (PDF)

AUTHOR INFORMATION

Corresponding Authors

Kasper Wenderich − *MESA+ Institute, Photocatalytic Synthesis Group, University of Twente, 7500 AE Enschede, The Netherlands;* ⓞ orcid.org/0000-0003-4767-8786; Email: k.wenderich@utwente.nl

Bastian T. Mei − *MESA+ Institute, Photocatalytic Synthesis Group, University of Twente, 7500 AE Enschede, The Netherlands;* ⓞ orcid.org/0000-0002-3973-9254; Email: b.t.mei@utwente.nl

Authors

Birgit A. M. Nieuweweme − *MESA+ Institute, Photocatalytic Synthesis Group, University of Twente, 7500 AE Enschede, The Netherlands*

Guido Mul − *MESA+ Institute, Photocatalytic Synthesis Group, University of Twente, 7500 AE Enschede, The Netherlands;* ⓞ orcid.org/0000-0001-5898-6384

Complete contact information is available at:
https://pubs.acs.org/10.1021/acssuschemeng.1c01244

Author Contributions

The manuscript was written through contributions of all authors. All authors have given approval to the final version of the manuscript.

Notes

The authors declare no competing financial interest.

ABBREVIATIONS

AEM, anion-exchange membrane; AO, anthraquinone oxidation; BDD, boron-doped diamond; BoS, balance of systems; CAPEX, capital expenditures; CFP, carbon fiber paper; CV, cyclic voltammetry; DSA, dimensionally stable anode(s); FE, Faradaic efficiency; GC, glassy carbon; HER, hydrogen evolution reaction; HP, hydrogen peroxide; HPER, hydrogen peroxide evolution reaction; LCH, levelized cost of hydrogen; MEA, membrane electrode assembly; NPV, net present value; OPEX, operating expenditures; PEC, photoelectrochemical; PTFE, polytetrafluoroethylene; PV, photovoltaic(s); PV-E, photovoltaic-electrolysis; RHE, reference hydrogen electrode; SEM, scanning electron microscopy; SMR, steam methane reforming; STH efficiency, solar-to-hydrogen efficiency

■ REFERENCES

(1) Shaner, M. R.; Atwater, H. A.; Lewis, N. S.; McFarland, E. W. A comparative technoeconomic analysis of renewable hydrogen production using solar energy. *Energy Environ. Sci.* **2016**, *9*, 2354−2371.

(2) Carmo, M.; Fritz, D. L.; Mergel, J.; Stolten, D. A comprehensive review on PEM water electrolysis. *Int. J. Hydrogen Energy* **2013**, *38*, 4901−4934.

(3) Turner, J. A. Sustainable hydrogen production. *Science* **2004**, *305*, 972−974.

(4) Jia, J.; Seitz, L. C.; Benck, J. D.; Huo, Y.; Chen, Y.; Ng, J. W. D.; Bilir, T.; Harris, J. S.; Jaramillo, T. F. Solar water splitting by photovoltaic-electrolysis with a solar-to-hydrogen efficiency over 30%. *Nat. Commun.* **2016**, *7*, 13237.

(5) Turner, J.; Sverdrup, G.; Mann, M. K.; Maness, P.-C.; Kroposki, B.; Ghirardi, M.; Evans, R. J.; Blake, D. Renewable hydrogen production. *Int. J. Energy Res.* **2008**, *32*, 379−407.

(6) Holladay, J. D.; Hu, J.; King, D. L.; Wang, Y. An overview of hydrogen production technologies. *Catal. Today* **2009**, *139*, 244−260.

(7) Abbasi, T.; Abbasi, S. A. 'Renewable' hydrogen: Prospects and challenges. *Renewable Sustainable Energy Rev.* **2011**, *15*, 3034−3040.

(8) Grimm, A.; de Jong, W. A.; Kramer, G. J. Renewable hydrogen production: A techno-economic comparison of photoelectrochemical cells and photovoltaic-electrolysis. *Int. J. Hydrogen Energy* **2020**, *45*, 22545−22555.

(9) Kudo, A.; Miseki, Y. Heterogeneous photocatalyst materials for water splitting. *Chem. Soc. Rev.* **2009**, *38*, 253−278.

(10) Osterloh, F. E. Inorganic nanostructures for photoelectrochemical and photocatalytic water splitting. *Chem. Soc. Rev.* **2013**, *42*, 2294−2320.

(11) Hisatomi, T.; Kubota, J.; Domen, K. Recent advances in semiconductors for photocatalytic and photoelectrochemical water splitting. *Chem. Soc. Rev.* **2014**, *43*, 7520−7535.

(12) Mei, B.; Mul, G.; Seger, B. Beyond water splitting: Efficiencies of photo-electrochemical devices producing hydrogen and valuable oxidation products. *Adv. Sustainable Syst.* **2017**, *1*, 1600035.

(13) Campos-Martin, J. M.; Blanco-Brieva, G.; Fierro, J. L. G. Hydrogen peroxide synthesis: An outlook beyond the anthraquinone process. *Angew. Chem., Int. Ed.* **2006**, *45*, 6962−6984.

(14) Ciriminna, R.; Albanese, L.; Meneguzzo, F.; Pagliaro, M. Hydrogen peroxide: A key chemical for today's sustainable development. *ChemSusChem* **2016**, *9*, 3374−3381.

(15) Yang, S.; Verdaguer-Casadevall, A.; Arnarson, L.; Silvioli, L.; Čolić, V.; Frydendal, R.; Rossmeisl, J.; Chorkendorff, I.; Stephens, I. E. L. Toward the decentralized electrochemical production of H_2O_2: A focus on the catalysis. *ACS Catal.* **2018**, *8*, 4064−4081.

(16) Jiang, Y.; Ni, P.; Chen, C.; Lu, Y.; Yang, P.; Kong, B.; Fisher, A.; Wang, X. Selective electrochemical H_2O_2 production through two-electron oxygen electrochemistry. *Adv. Energy Mater.* **2018**, *8*, 1801909.

(17) Goor, G.; Glenneberg, J.; Jacobi, S.; Dadabhoy, J.; Candido, E. Hydrogen peroxide. *Ullmann's Encyclopedia of Industrial Chemistry*, 2019; pp 1−40.

(18) Fukuzumi, S.; Yamada, Y.; Karlin, K. D. Hydrogen peroxide as a sustainable energy carrier: Electrocatalytic production of hydrogen peroxide and the fuel cell. *Electrochim. Acta* **2012**, *82*, 493−511.

(19) Samanta, C. Direct synthesis of hydrogen peroxide from hydrogen and oxygen: An overview of recent developments in the process. *Appl. Catal., A* **2008**, *350*, 133−149.

(20) Sayama, K. Production of high-value-added chemicals on oxide semiconductor photoanodes under visible light for solar chemical-conversion processes. *ACS Energy Lett.* **2018**, *3*, 1093−1101.

(21) Perry, S. C.; Pangotra, D.; Vieira, L.; Csepei, L.-I.; Sieber, V.; Wang, L.; Ponce de León, C.; Walsh, F. C. Electrochemical synthesis of hydrogen peroxide from water and oxygen. *Nat. Rev. Chem.* **2019**, *3*, 442−458.

(22) Xia, C.; Back, S.; Ringe, S.; Jiang, K.; Chen, F.; Sun, X.; Siahrostami, S.; Chan, K.; Wang, H. Confined local oxygen gas promotes electrochemical water oxidation to hydrogen peroxide. *Nat. Catal.* **2020**, *3*, 125−134.

(23) Eul, W.; Moeller, A.; Steiner, N. Hydrogen peroxide. *Kirk-Othmer Encyclopedia of Chemical Technology*, 2001; Vol. *13*, pp 1−58.

(24) Berl, E. A new cathodic process for the production of H_2O_2. *Trans. Electrochem. Soc.* **1939**, *76*, 359−369.

(25) Foller, P. C.; Bombard, R. T. Processes for the production of mixtures of caustic soda and hydrogen peroxide via the reduction of oxygen. *J. Appl. Electrochem.* **1995**, *25*, 613−627.

(26) HPNow. https://www.hpnow.eu/ (accessed Feb 2021).

(27) Fukuzumi, S.; Lee, Y. M.; Nam, W. Solar-driven production of hydrogen peroxide from water and dioxygen. *Chem.—Eur. J.* **2018**, *24*, 5016−5031.

(28) Liu, J.; Zou, Y.; Jin, B.; Zhang, K.; Park, J. H. Hydrogen peroxide production from solar water oxidation. *ACS Energy Lett.* **2019**, *4*, 3018−3027.

(29) Mavrikis, S.; Perry, S. C.; Leung, P. K.; Wang, L.; Ponce de León, C. Recent advances in electrochemical water oxidation to produce hydrogen peroxide: A mechanistic perspective. *ACS Sustainable Chem. Eng.* **2021**, *9*, 76−91.

(30) Shi, X.; Back, S.; Gill, T. M.; Siahrostami, S.; Zheng, X. Electrochemical synthesis of H_2O_2 by two-electron water oxidation reaction. *Chem* **2021**, *7*, 38−63.

(31) Xue, Y.; Wang, Y.; Pan, Z.; Sayama, K. Electrochemical and photoelectrochemical water oxidation for hydrogen peroxide production. *Angew. Chem., Int. Ed.* **2021**, *60*, 10469−10480.

(32) Fuku, K.; Miyase, Y.; Miseki, Y.; Gunji, T.; Sayama, K. Enhanced oxidative hydrogen peroxide production on conducting glass anodes modified with metal oxides. *ChemistrySelect* **2016**, *1*, 5721−5726.

(33) Shi, X.; Siahrostami, S.; Li, G.-L.; Zhang, Y.; Chakthranont, P.; Studt, F.; Jaramillo, T. F.; Zheng, X.; Nørskov, J. K. Understanding activity trends in electrochemical water oxidation to form hydrogen peroxide. *Nat. Commun.* **2017**, *8*, 701.

(34) Fuku, K.; Sayama, K. Efficient oxidative hydrogen peroxide production and accumulation in photoelectrochemical water splitting using a tungsten trioxide/bismuth vanadate photoanode. *Chem. Commun.* **2016**, *52*, 5406−5409.

(35) Fuku, K.; Miyase, Y.; Miseki, Y.; Funaki, T.; Gunji, T.; Sayama, K. Photoelectrochemical hydrogen peroxide production from water on a $WO_3/BiVO_4$ photoanode and from O_2 on an Au cathode without external bias. *Chem.—Asian J.* **2017**, *12*, 1111−1119.

(36) Fuku, K.; Miyase, Y.; Miseki, Y.; Gunji, T.; Sayama, K. $WO_3/BiVO_4$ photoanode coated with mesoporous Al_2O_3 layer for oxidative production of hydrogen peroxide from water with high selectivity. *RSC Adv.* **2017**, *7*, 47619−47623.

(37) Miyase, Y.; Takasugi, S.; Iguchi, S.; Miseki, Y.; Gunji, T.; Sasaki, K.; Fujita, E.; Sayama, K. Modification of $BiVO_4/WO_3$ composite photoelectrodes with Al_2O_3 via chemical vapor deposition for highly efficient oxidative H_2O_2 production from H_2O. *Sustainable Energy Fuels* **2018**, *2*, 1621−1629.

(38) Jeon, T. H.; Kim, H.; Kim, H.-i.; Choi, W. Highly durable photoelectrochemical H_2O_2 production via dual photoanode and cathode processes under solar simulating and external bias-free conditions. *Energy Environ. Sci.* **2020**, *13*, 1730−1742.

(39) Baek, J. H.; Gill, T. M.; Abroshan, H.; Park, S.; Shi, X.; Nørskov, J.; Jung, H. S.; Siahrostami, S.; Zheng, X. Selective and efficient Gd-doped $BiVO_4$ photoanode for two-electron water oxidation to H_2O_2. *ACS Energy Lett.* **2019**, *4*, 720−728.

(40) Miyase, Y.; Iguchi, S.; Miseki, Y.; Gunji, T.; Sayama, K. Electrochemical H_2O_2 production and accumulation from H_2O by composite effect of Al_2O_3 and $BiVO_4$. *J. Electrochem. Soc.* **2019**, *166*, H644−H649.

(41) Izgorodin, A.; Izgorodina, E.; MacFarlane, D. R. Low overpotential water oxidation to hydrogen peroxide on a MnO_x catalyst. *Energy Environ. Sci.* **2012**, *5*, 9496−9501.

(42) Park, S. Y.; Abroshan, H.; Shi, X.; Jung, H. S.; Siahrostami, S.; Zheng, X. $CaSnO_3$: An electrocatalyst for two-electron water oxidation reaction to form H_2O_2. *ACS Energy Lett.* **2019**, *4*, 352−357.

(43) Kelly, S. R.; Shi, X.; Back, S.; Vallez, L.; Park, S. Y.; Siahrostami, S.; Zheng, X.; Nørskov, J. K. ZnO as an active and selective catalyst for electrochemical water oxidation to hydrogen peroxide. *ACS Catal.* **2019**, *9*, 4593−4599.

(44) Xue, S.-g.; Tang, L.; Tang, Y.-k.; Li, C.-x.; Li, M.-l.; Zhou, J.-j.; Chen, W.; Zhu, F.; Jiang, J. Selective electrocatalytic water oxidation to produce H_2O_2 using a C,N codoped TiO_2 electrode in an acidic electrolyte. *ACS Appl. Mater. Interfaces* **2020**, *12*, 4423−4431.

(45) Shiragami, T.; Nakamura, H.; Matsumoto, J.; Yasuda, M.; Suzuri, Y.; Tachibana, H.; Inoue, H. Two-electron oxidation of water to form hydrogen peroxide sensitized by di(hydroxo)porphyrin Ge^{IV} complex under visible-light irradiation. *J. Photochem. Photobiol., A* **2015**, *313*, 131−136.

(46) Kuttassery, F.; Mathew, S.; Sagawa, S.; Remello, S. N.; Thomas, A.; Yamamoto, D.; Onuki, S.; Nabetani, Y.; Tachibana, H.; Inoue, H. One electron-initiated two-electron oxidation of water by aluminum porphyrins with earth's most abundant metal. *ChemSusChem* **2017**, *10*, 1909−1915.

(47) Cobb, S. J.; Ayres, Z. J.; Macpherson, J. V. Boron doped diamond: A designer electrode material for the twenty-first century. *Annu. Rev. Anal. Chem.* **2018**, *11*, 463−484.

(48) McCreery, R. L. Advanced carbon electrode materials for molecular electrochemistry. *Chem. Rev.* **2008**, *108*, 2646−2687.

(49) Asadian, E.; Ghalkhani, M.; Shahrokhian, S. Electrochemical sensing based on carbon nanoparticles: A review. *Sens. Actuators, B* **2019**, *293*, 183−209.

(50) Yang, N.; Foord, J. S.; Jiang, X. Diamond electrochemistry at the nanoscale: A review. *Carbon* **2016**, *99*, 90−110.

(51) Mavrikis, S.; Göltz, M.; Rosiwal, S.; Wang, L.; Ponce de León, C. Boron-doped diamond electrocatalyst for enhanced anodic H_2O_2 production. *ACS Appl. Energy Mater.* **2020**, *3*, 3169−3173.

(52) Wenderich, K.; Kwak, W.; Grimm, A.; Kramer, G. J.; Mul, G.; Mei, B. Industrial feasibility of anodic hydrogen peroxide production through photoelectrochemical water splitting: a techno-economic analysis. *Sustainable Energy Fuels* **2020**, *4*, 3143−3156.

(53) Qiang, Z.; Chang, J.-H.; Huang, C.-P. Electrochemical generation of hydrogen peroxide from dissolved oxygen in acidic solutions. *Water Res.* **2002**, *36*, 85−94.

(54) Pinaud, B. A.; Benck, J. D.; Seitz, L. C.; Forman, A. J.; Chen, Z.; Deutsch, T. G.; James, B. D.; Baum, K. N.; Baum, G. N.; Ardo, S.; Wang, H.; Miller, E.; Jaramillo, T. F. Technical and economic feasibility of centralized facilities for solar hydrogen production via photocatalysis and photoelectrochemistry. *Energy Environ. Sci.* **2013**, *6*, 1983−2002.

(55) James, B. D.; Baum, G. N.; Perez, J.; Baum, K. N. *Technoeconomic Analysis of Photoelectrochemical (PEC) Hydrogen Production*; Directed Technologies Inc.: Arlington, Virginia, 2009.

(56) EnergyTrend. https://www.energytrend.com/solar-price.html (accessed Nov 2020).

(57) ICIS. www.icis.com/chemicals (accessed Jan 2017).

(58) International Technology Roadmap for Photovoltaic (ITRPV)—2019 Results; VDMA: April 2020.

(59) The base-case costs have been estimated after discussion with Condias GmbH, a German company specialized in the production of polycrystalline diamond coatings. A worst-case scenario is estimated when both sides of the substrate need to be coated with BDD, whereas a best-case scenario is estimated when only one side of the substrate needs to be coated with BDD. The average is the base-case costs.

(60) Luong, J. H. T.; Male, K. B.; Glennon, J. D. Boron-doped diamond electrode: synthesis, characterization, functionalization and analytical applications. *Analyst* **2009**, *134*, 1965−1979.

(61) Macpherson, J. V. A practical guide to using boron doped diamond in electrochemical research. *Phys. Chem. Chem. Phys.* **2015**, *17*, 2935−2949.

(62) Łukaszewski, M.; Soszko, M.; Czerwiński, A. Electrochemical methods of real surface area determination of noble metal electrodes − an overview. *Int. J. Electrochem. Sci.* **2016**, *11*, 4442−4469.

(63) Morales, D. M.; Risch, M. Seven steps to reliable cyclic voltammetry measurements for the determination of double layer capacitance. *J. Phys. Energy* **2021**, DOI: 10.1088/2515-7655/abee33. , in press

(64) These costs have been estimated after discussion with MAGNETO special anodes B.V. (an Evoqua brand). The costs are based on a Ti plate coated on one side with an Ir-based coating.

(65) FuelCellStore. https://www.fuelcellstore.com (accessed Apr 2021).

(66) Möller, S.; Barwe, S.; Masa, J.; Wintrich, D.; Seisel, S.; Baltruschat, H.; Schuhmann, W. Online monitoring of electrochemical carbon corrosion in alkaline electrolytes by differential electrochemical mass spectrometry. *Angew. Chem., Int. Ed.* **2020**, *59*, 1585−1589.

(67) Chardon, C. P.; Matthée, T.; Neuber, R.; Fryda, M.; Comninellis, C. Efficient electrochemical production of peroxodicarbonate applying DIACHEM® diamond electrodes. *ChemistrySelect* **2017**, *2*, 1037−1040.